Two-Step Sequential Detection in Agile-Beam Radars: Performance and Tradeoffs

EMANUELE GROSSI , Senior Member, IEEE
MARCO LOPS , Senior Member, IEEE
LUCA VENTURINO, Senior Member, IEEE
Università degli Studi di Cassino e del Lazio Meridionale, Cassino, Italy

In this paper, we consider a surveillance radar equipped with an electronically scanned antenna and study the performance of a two-step sequential detection procedure, where, for each resolution cell, a second observation is taken if a reliable decision cannot be made after the first one. At the design stage, we optimize the available degrees of freedom (namely, dwell time and detection thresholds) so as to maximize the detection rate (DR), defined as the average number of detections from a target per unit of time, under a constraint on the false alarm rate (FAR), which is the average number of false alarms per unit of time from the inspected area. This is motived by the fact that DR and FAR, beside of being *per se* meaningful figures of merit for parameter tuning, allow a fair performance comparison among detection strategies with different scanning policies. Examples are presented to illustrate the effects of this design philosophy under the two relevant situations of a slowly fluctuating and a fast-fluctuating target response, also in the presence of clutter.

I. INTRODUCTION

Surveillance radar systems constantly monitor a given region for timely threat prevention [1]–[3]. A newly born target should be detected in several consecutive scans before an automatic track initiation is started or an action is taken by the human operator [4], [5]. In traditional (e.g., mechanical) systems adopting a uniform scanning policy, for a fixed probability of false alarm, the probability of detection in each scan (also known as single-scan detection probability or blip/scan ratio [6]) can be improved by reducing the angular velocity of the rotating antenna so as to increase the dwell time and, consequently, the time-on-target; however, a longer scan duration increases the time elapsing between successive hits from the same target, thus increasing the reaction time of the radar [7]. In [8], Billam recognized the importance of *getting around the sky quick enough* and showed that the scan duration is connected to the maximum penetration range of an undetected target inside the covered area. The efficient management of the time resource is, therefore, a key challenge in the system design, especially for multifunction radars, that must be capable of simultaneously supporting numerous and potentially conflicting tasks [9]–[12]. Recently, this concept has been put forward in [13], wherein dwell time and detection threshold are jointly chosen so as to maximize the detection rate (DR), defined as the average number of detections per unit of time from a target, under a constraint on the false alarm rate (FAR), defined as the average number of false alarms per unit of time from the inspected area. Indeed, a larger DR implies a shorter time interval between consecutive hits from a persistent target or a faster discovery of a newly born target; also, a larger DR may facilitate subsequent track-before-detect [14]–[22] and/or tracking [4], [23]–[26] algorithms, since more frequent hits result in a smaller association gate in the track estimation process. On the other hand, FAR is commonly adopted by radar engineers to measure whether a radar is troubled by excessive false alarms; in particular, it has a direct impact on the computational requirement for real-time data processing and on the capacity of the human operator to take actions by monitoring the hits visualized on the radar scope [1], [27]. Intuitively, under this design framework, the optimal detection threshold increases with the scan rate, as fewer false alarms can be tolerated in each scan, while the optimal dwell time depends upon the signal-to-clutter-plus-noise ratio (SCNR), as stronger targets can be detected in a shorter time.

Radars equipped with an electronically scanned antenna offer additional degrees of freedom for system design due to their agile beam-steering capability, which allows us to implement more advanced scanning policies [2], [4], [28]–[30]. In this context, sequential detection procedures can be adopted to improve the radar detection capability compared to fixed-sample-size tests [31]–[46]. To avoid the problem of hanging up in a given beam direction for long time, truncated sequential procedures are employed in practice [47]–[51]. A common method, called energy-variant sequential detection or alert-and-confirm

detection (ACD) [28], [30], [52]–[55], assumes that the radar searches the whole volume and compares the returns from each resolution cell to a threshold: Every time the threshold is crossed (alert), a second look is requested to make a definite decision (confirm). Previous works on ACD focused on the probability of detection or the cumulative probability of detection, the latter measuring the capability of a search radar to detect a newly born target within a preassigned time interval, showing that a sensitivity improvement of several decibels is possible over traditional fixed-sample-size detection (FXD)[1] under a constraint on the probability of false alarm. However, this analysis appears unfair, as it does not account for the fact that ACD and FXD present a different measurement update interval, whereby the improved sensitivity might come at the price of a longer scan time; also, no previous work has provided a comparative study between ACD and a more intuitive procedure, where a second look is requested only if a reliable decision cannot be made after the first observation.

In this paper we consider a two-step sequential detection (TSD) procedure, where the statistic from each resolution cell is compared to an upper and a lower threshold: If the upper threshold is crossed a detection is declared, while the statistics falling in between the two thresholds are deemed as *alerts*, which must be revisited through a second look to make a definite decision.[2] Starting from preliminary results in [57], we investigate the value of this strategy in surveillance radars when time is a resource at stake included in the system design. We choose a rather general framework, wherein the second look can be taken immediately after the first one or be delayed, so as to encompass the cases of both a slowly fluctuating target (SFT) and a fast-fluctuating target (FFT). Following [13], we consider DR and FAR for system design and analysis, as they allow a fair comparison among detection strategies adopting scanning policies with a different scan time. After deriving a closed-form expression for these metrics, DR is maximized over the available degrees of freedom (namely, the dwell time and the detection thresholds) under a constraint on FAR. Our results reveal that TSD yields a negligible DR improvement as compared to FXD in the extremely low and extremely high SCNR regimes. In all other cases, sensitivity gains up to 2.8 dB have been observed in our examples, depending on the operating conditions. Interestingly, the sensitivity gain granted by TSD over FXD increases when the desired FAR level or the number of inspected range cells are reduced. Also, TSD is generally more rewarding for SFT and in the clutter limited regime. Finally, we found that ACD can be much worse than TSD, as forcing the radar to declare each detection after two looks results in a less efficient use of the time resource.

The remainder of this paper is organized as follows. In Section II, the system model and the detection strategy are described. In Section III, system optimization is discussed and closed-form expressions of FAR, DR, and average scan time are derived. In Section IV, a thorough performance assessment is provided. Finally, concluding remarks are given in Section V.

II. SYSTEM DESCRIPTION

We consider a pulse radar observing an angular sector composed of $N_a \in \mathbb{N}$ azimuth bins (whose size is tied to the beam-width of the transmit antenna) and $N_r \in \mathbb{N}$ range bins (whose size is tied to the bandwidth of the transmit waveform). The transmitted signal is a pulse train with pulse repetition time T, and the received signal undergoes a standard processing chain, which may involve passband-to-baseband conversion, digitalization, range gating, constant false alarm rate processing, clutter mitigation, and pulse integration.

TSD is a truncated sequential detection procedure with terminal stage equal to two, so that either one or two observations are taken from each resolution cell. We assume here that the first observation is based on the elaboration of $M_1 \in \mathbb{N}$ pulses, emitted in each azimuth direction, while the second comes from the elaboration of $M_2 \in \mathbb{N}$ pulses, emitted only in those azimuth directions containing range bins for which no reliable decision can be made after the first observation. The second observation (whenever needed) can be taken in several moments of the scan, the two extreme cases being the following. On the one side, for each azimuth direction, the second look is taken immediately after the first one, before rotating the antenna beam toward the next azimuth direction: We refer to this method as *short-time interleaving*. On the other side, the whole area under surveillance is uniformly scanned (by rotating the antenna beam at a constant angular velocity), and then the antenna beam is steered toward each azimuth direction that contains range bins requiring a second look: We refer to this method as *long-time interleaving*. In any case, the scan time is

$$T_s = N_a M_1 T + K M_2 T \qquad (1)$$

where K is the number of revisited azimuth directions, a random variable taking on values in the set $\{0, 1, \ldots, N_a\}$.

Let H_0 denote the hypothesis that the target is not present in the range-azimuth cell under test, and let H_1 denote its alternative; also, let $y_1 \geq 0$ and $y_2 \geq 0$ be the statistics obtained in the first and second (if any) observation of the cell under test, respectively. Then the test is[3]

$$y_1 \begin{cases} < a, & \text{declare } H_0 \\ \geq b, & \text{declare } H_1 \\ \in [a, b), & \text{take a second observation and} \end{cases}$$

$$\qquad\qquad y_2 \begin{cases} < \eta, & \text{declare } H_0 \\ \geq \eta, & \text{declare } H_1 \end{cases} \qquad (2)$$

---

[1]The name is derived from the fact that the decision is based on a sample of fixed length, i.e., on a single look. Since azimuth sectors are revisited at a constant rate, we may also refer to it as uniform-scanning detection.

[2]A similar scanning policy is considered in [56], but only the upper threshold is used to validate the first observation, and a fixed number of resolution cells with statistics falling below this threshold (selected according to a heuristic rule) are revisited.

[3]We are implicitly assuming that the test statistic comes from an integration process (either coherent or incoherent), so that the hypothesis H_1 becomes more and more likely as the test statistic increases.

where $0 \leq a \leq b$ are the boundaries of the sequential test, and $\eta \geq 0$ is the final threshold.

We are assuming here that range/azimuth migration of a prospective target between the two looks can be neglected. The validity of this assumption highly depends on the radar (range/azimuth bin width) and target (position and velocity) characteristics, but, even for fast moving targets and small range/azimuth bins, it could be verified with short-time interleaving and sufficiently small values of M_1 and M_2. The critical situation of large pulse train lengths and/or long-time interleaving with fast moving-targets and high-resolution radars can be handled by elaborating in the second look a group of adjacent resolution cells around the one under inspection [58]. Notice also that this detection strategy subsumes FXD when $b = a$, since the interval $[a, b]$ degenerates to the empty set, and a second look is never requested. When, instead, $b = \infty$, TSD reduces to ACD in [28], [52]–[55], and the second look is always taken. In the following, we assume that, for ACD, b can be set equal to either a or ∞, so that even ACD subsumes FXD as a special case.

III. SYSTEM OPTIMIZATION

The available degrees of freedom for system optimization are the thresholds (a, b, η) and the number of processed pulses (M_1, M_2). Following [13], we propose to maximize DR under a constraint on FAR, i.e.,

$$\begin{array}{cl} \max_{\substack{M_1, M_2 \in \mathcal{M} \\ b \geq a \geq 0, \eta \geq 0}} & \mathrm{DR}(a, b, \eta, M_1, M_2) \\ \text{s.t.} & \mathrm{FAR}(a, b, \eta, M_1, M_2) \leq \mathrm{FAR}_{\max} \end{array} \quad (3)$$

where $\mathcal{M}$ is the finite set of possible pulse train lengths (tied to the target mobility and/or to the maximum time lag allowed between successive measurements), whose minimum and maximum are denoted $M_{\min}$ and $M_{\max}$, respectively, while $\mathrm{FAR}_{\max} \in \left(0, N_r/(M_{\min}T)\right)$ is the maximum FAR level[4] that can be tolerated (tied to the computational requirement for real-time data processing and/or to the capacity of the human operator to take actions by monitoring the hits visualized on the radar scope).

Next, we provide closed-form expressions of FAR and DR: The former is computed when no target is present in the whole inspected area, this hypothesis being denoted H_0^*, and the latter when a single target is present in the scene at a random position, this hypothesis being denoted H_1^*. Also, we assume that the test statistics from different cells are independent and, under H_0, identically distributed. The goal here is to capture the main performance trade-offs while maintaining the mathematical problem tractable. For the sake of notational compactness, the dependence on (a, b, η, M_1, M_2) will not be stated explicitly. Under these assumptions, we have

$$\mathrm{FAR} = \begin{cases} \sum_{k=0}^{N_a} \dfrac{\left(N_r N_a - \frac{k N_r p}{1-(1-p)^{N_r}}\right) \frac{P_{\mathrm{fa},1}}{1-p} + \frac{k N_r P_{\mathrm{fa},2}}{1-(1-p)^{N_r}}}{N_a M_1 T + k M_2 T} \\ \quad \times \binom{N_a}{k} \left(1 - (1-p)^{N_r}\right)^k (1-p)^{N_r(N_a-k)} \\ \qquad \text{if } p \in (0, 1) \\ \dfrac{N_r P_{\mathrm{fa},1}}{M_1 T}, \qquad \text{if } p = 0 \\ \dfrac{N_r P_{\mathrm{fa}}}{(M_1 + M_2)T}, \quad \text{if } p = 1 \end{cases} \quad (4)$$

where

$$P_{\mathrm{fa},1} = \Pr\left(y_1 \geq \gamma_{\mathrm{up}} \mid H_0\right) \quad (5a)$$
$$P_{\mathrm{fa},2} = \Pr\left(y_1 \in [\gamma_{\mathrm{low}}, \gamma_{\mathrm{up}}), y_2 \geq \eta \mid H_0\right) \quad (5b)$$
$$p = \Pr\left(y_1 \in [\gamma_{\mathrm{low}}, \gamma_{\mathrm{up}}) \mid H_0\right) \quad (5c)$$

are the probabilities of having a false alarm in the first look, having a false alarm in the second look, and revisiting a noise-only cell, respectively, and $P_{\mathrm{fa}} = P_{\mathrm{fa},1} + P_{\mathrm{fa},2}$ is the probability of false alarm. The proof of (4) is reported in Section A of the Appendix. Furthermore, we have

$$\mathrm{DR} = \begin{cases} \sum_{k=0}^{N_a-1} \left(\dfrac{P_{\mathrm{d},1}(1-p)^{N_r-1}}{N_a M_1 T + k M_2 T} \right. \\ \left. + \dfrac{P_{\mathrm{d},1}\left(1 - (1-p)^{N_r-1}\right) + P_{\mathrm{d},2}}{N_a M_1 T + (k+1)M_2 T} \right) \\ \quad \times \binom{N_a-1}{k} \left(1 - (1-p)^{N_r}\right)^k (1-p)^{N_r(N_a-1-k)}, \\ \qquad \text{if } p \in (0, 1) \\ \dfrac{P_{\mathrm{d},1}}{N_a M_1 T} + \dfrac{P_{\mathrm{d},2}}{N_a M_1 T + M_2 T}, \\ \qquad \text{if } p = 0 \\ \dfrac{P_{\mathrm{d},1}}{N_a M_1 T + (N_a-1)M_2} + \dfrac{P_{\mathrm{d},2}}{N_a(M_1 + M_2)T}, \\ \qquad \text{if } p = 1 \text{ and } N_r = 1 \\ \dfrac{P_{\mathrm{d}}}{N_a(M_1 + M_2)T}, \qquad \text{if } p = 1 \text{ and } N_r \geq 2 \end{cases} \quad (6)$$

where

$$P_{\mathrm{d},1} = \Pr(y_1 \geq \gamma_{\mathrm{up}} \mid H_1) \quad (7a)$$
$$P_{\mathrm{d},2} = \Pr\left(y_1 \in [\gamma_{\mathrm{low}}, \gamma_{\mathrm{up}}), y_2 \geq \eta \mid H_1\right) \quad (7b)$$

are the probabilities of detecting the target in the first look and in the second look, respectively, and $P_{\mathrm{d}} = P_{\mathrm{d},1} + P_{\mathrm{d},2}$ is the probability of detection. The proof of (6) is reported in Section B of the Appendix.

Notice in passing that the average scan time under H_0^* and H_1^* is

$$\mathrm{AST}_{H_0^*} = N_a M_1 T + N_a \left(1 - (1-p)^{N_r}\right) M_2 T \quad (8a)$$
$$\begin{aligned} \mathrm{AST}_{H_1^*} = N_a M_1 T + &\left[N_a \left(1 - (1-p)^{N_r}\right) \right. \\ &\left. + (q - p)(1-p)^{N_r-1}\right] M_2 T \end{aligned} \quad (8b)$$

where

$$q = \Pr\left(y_1 \in [\gamma_{\mathrm{low}}, \gamma_{\mathrm{up}}) \mid H_1\right) \quad (9)$$

is the probability of revisiting the resolution bin containing the target. The proof of (8) is reported in Section C of the Appendix.

IV. PERFORMANCE ANALYSIS

We consider here an additive signal model with Swerling I target fluctuation, K-distributed clutter, and

---

[4] Notice that the lowest possible FAR is zero, obtained with a zero probability of false alarm, while the largest possible FAR is $N_r/(M_{\min}T)$, obtained with a probability of false alarm equal to one, so as to have $N_r N_a$ false alarms in a scan, and $T_s = N_a M_{\min}T$.

Gaussian noise, and assume coherent integration of the pulses at the receiver. Specifically, the test statistic is

$$y_i = \begin{cases} \left| \sqrt{M_i \rho_s} s_i + \sqrt{M_i \rho_c \tau} c_i + n_i \right|^2, & \text{under } H_1 \\ \left| \sqrt{M_i \rho_c \tau} c_i + n_i \right|^2, & \text{under } H_0 \end{cases}$$

(10)

for $i = 1, 2$, where: s_i, c_i, and n_i are unit-variance complex circularly-symmetric Gaussian random variables representing the target response, the speckle component of the clutter, and the noise, respectively; τ is a unit-mean Γ-distributed random variable, with shape parameter ν and scale parameter $1/\nu$, representing the texture of the clutter; and ρ_s and ρ_c are the signal-to-noise ratio (SNR) and the clutter-to-noise ratio (CNR) per pulse, respectively. The variables $\{s_1, c_1, c_2, \tau, n_1, n_2\}$ are independent; also, s_2 is either equal to s_1 or independent of $\{s_1, c_1, c_2, \tau, n_1, n_2\}$: The former models the SFT case, where the target response remains constant during the two observations in the same scan (this is usually verified in short-time interleaving), while the latter models the FFT case, where the target response changes at every observation (this may be verified in long-time interleaving or in the presence of frequency agility).

Under the model in (10), the probabilities in (5) take the following form:

$$P_{\text{fa},1} = \int_0^\infty e^{\frac{-b}{1+xM_1\rho_c}} f(x)dx \tag{11a}$$

$$P_{\text{fa},2} = \int_0^\infty e^{\frac{-\eta}{1+xM_2\rho_c}} \left(e^{\frac{-a}{1+xM_1\rho_c}} - e^{\frac{-b}{1+xM_1\rho_c}} \right) f(x)dx \tag{11b}$$

$$p = \int_0^\infty \left(e^{\frac{-a}{1+xM_1\rho_c}} - e^{\frac{-b}{1+xM_1\rho_c}} \right) f(x)dx \tag{11c}$$

where $f(x) = \frac{\nu^\nu}{\Gamma(\nu)} x^{\nu-1} e^{-\nu x} \mathbb{1}_{\{x \geq 0\}}$ is the probability density function of τ. Similarly, the probabilities in (7) and (9) are

$$P_{\text{d},1} = \int_0^\infty e^{\frac{-b}{1+xM_1\rho_c+M_1\rho_s}} f(x)dx \tag{12a}$$

$$P_{\text{d},2} = \begin{cases} \int_0^\infty e^{\frac{-\eta}{1+xM_2\rho_c+M_2\rho_s}} \\ \times \left(e^{\frac{-a}{1+xM_1\rho_c+M_1\rho_s}} - e^{\frac{-b}{1+xM_1\rho_c+M_1\rho_s}} \right) \\ \times f(x)dx, & \text{for SFT} \\ \int_0^\infty \int_0^\infty Q_1 \left(\sqrt{\frac{2yM_2\rho_s}{1+xM_2\rho_c}}, \sqrt{\frac{2\eta}{1+xM_2\rho_c}} \right) \\ \times \left[Q_1 \left(\sqrt{\frac{2yM_1\rho_s}{1+xM_1\rho_c}}, \sqrt{\frac{2a}{1+xM_1\rho_c}} \right) \right. \\ \left. - Q_1 \left(\sqrt{\frac{2yM_1\rho_s}{1+xM_1\rho_c}}, \sqrt{\frac{2b}{1+xM_1\rho_c}} \right) \right] \\ \times f(x)e^{-y}dxdy, & \text{for FFT} \end{cases}$$

(12b)

$$q = \int_0^\infty \left(e^{\frac{-a}{1+xM_1\rho_c+M_1\rho_s}} - e^{\frac{-b}{1+xM_1\rho_c+M_1\rho_s}} \right) f(x)dx \tag{12c}$$

where $Q_1(\cdot, \cdot)$ is the first-order Marqum Q-function.[5]

In the following, we study the performance of TSD, ACD, and FXD in two scenarios, namely, absence and presence of clutter ($\rho_c = 0$ and $\rho_c > 0$, respectively). All detection strategies are optimized according to (3), where, for ACD and FXD, the additional constraint $b \in \{a, \infty\}$ and $b = a$ is included, respectively.

A. Absence of Clutter

This may be the case of an air-search radar, where the antenna beam points toward the sky and does not collect reflections from the surrounding environment (noise-limited regime). For FXD, exploiting the results in [13], it can be verified that the mixed-integer nonlinear problem (3) has the following solution:

$$M_1^* = \begin{cases} M_{\min}, & \text{if } x^* \leq M_{\min} \\ M_{\max}, & \text{if } x^* \geq M_{\max} \\ \displaystyle\arg\max_{M_1 \in \{[x^*]_l, [x^*]_r\}} \frac{1}{M_1} \left(\frac{\text{FAR}_{\max} M_1 T}{N_r} \right)^{\frac{1}{1+M_1\rho_s}}, & \text{otherwise} \end{cases}$$

(13a)

$$b^* = -\ln \left(\frac{\text{FAR}_{\max} M_1^* T}{N_r} \right) \tag{13b}$$

where $x^* \in \left(0, N_r/(\text{FAR}_{\max} e T) \right)$ is the unique solution to[6]

$$\left(\frac{\text{FAR}_{\max} x T}{N_r} \right)^{\frac{1}{1+x\rho_s}} = \frac{1}{e} \tag{14}$$

and $[x^*]_l$ and $[x^*]_r$ are the left and right nearest neighbors of x^* in $\mathcal{M}$, respectively. It is seen from (13) that the optimal detection threshold must meet the FAR constraint with the equality sign, while the optimal number of integrated pulses attempts to provide a value of P_d approximately equal to $1/e$. Clearly, if the pair ($\text{FAR}_{\max}, \rho_s$) requires a value of x^* smaller than $M_{\min}$ or larger than $M_{\max}$ to (approximately) meet (14), then the value of P_d is necessarily larger or smaller than $1/e$, respectively (more on this in the following examples). For $b > a$, obtaining a closed-form expression for the solution of (3) appears unfeasible; hence, we resort to numerical evaluation. In the following, we set $T = 1$ ms and $\mathcal{M} = \{8m\}_{m=1}^8$, and analyze the optimized DR and the corresponding system parameters. DR and FAR are expressed in detections per minute (det/min) and false alarms per minute (fa/min), respectively.

Fig. 1 shows the optimized DR as a function of ρ_s when $N_a = 40$, $N_r = 1000$, and $\text{FAR}_{\max} = 0.5$ fa/min. As expected, TSD outperforms FXD, while ACD remains in between: This is a consequence of the fact that, by definition, ACD is a special case of TSD and subsumes FXD. All curves present an S-shaped monotonic growth and converge to the asymptotic maximum value $1/(N_a M_{\min} T)$ for $\rho_s \to \infty$, as a consequence of the fact that $P_d \to 1$. Also, all curves are lower bounded by $\text{FAR}_{\max}/(N_r N_a)$, which is the asymptotic DR value for FXD in the limit that $\rho_s \to 0$.

---

[5]Note that the probabilities in (11) and (12), and, therefore, FAR and DR, depend on ρ_c and ρ_s, which are assumed known to solve (3). If ρ_c and ρ_s are not known, then, as typical in sequential detection, they can be set at some design values, and losses are accepted in case of mismatch.

[6]The left-hand side of (14) is the probability of detection evaluated at $b = a = b^*$, once the integer variable M_1 is relaxed and replaced by the continuous variable x.
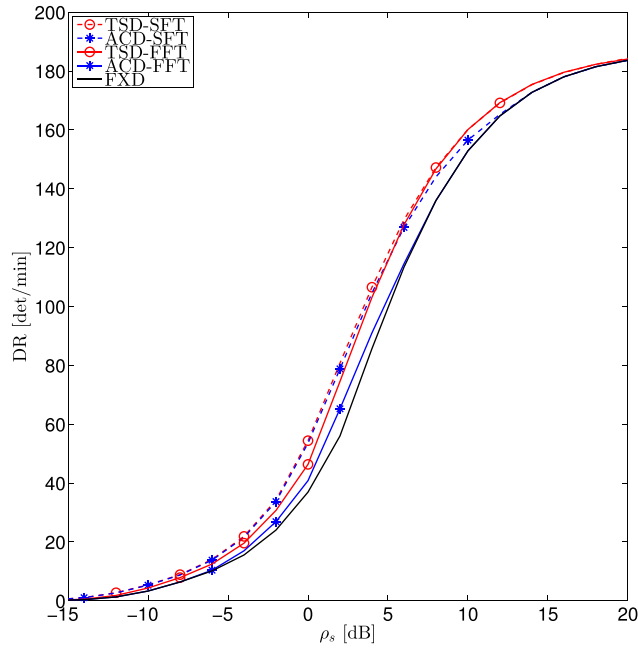
Fig. 1. Optimized DR versus SNR per pulse for TSD, ACD, and FXD when $N_a = 40$, $N_r = 1000$, $\text{FAR}_{\max} = 0.5$ fa/min, and $\rho_c = -\infty$ dB; both SFT and FFT are considered.

Interestingly, TSD is competitive with respect to FXD in the steep region of the S-shaped curve, which corresponds to ρ_s values in the range $[-10, 15]$ dB for the scenario considered here, while it provides a negligible advantage outside this region; also, the performance gap between the SFT and FFT models is here less than 0.5 dB for TSD, with the former being superior for small values of ρ_s (see also Figs. 7, 10, and 13, reported next, for more details). It should not surprise that the performance of TSD and ACD is close under the SFT model for small values of ρ_s, while it may significantly differ under the SFT model for large values of ρ_s or under the FFT model (at any ρ_s). Indeed, ACD suffers from the fact that an alert produced by a favorable response from a weak target is likely to be confirmed only if the same favorable response is reobserved in the second look; moreover, forcing the confirmation of strong targets results in an inefficient use of the time resource.

Fig. 2 shows, as a function of ρ_s, the values of P_d, P_{fa}, $\text{AST}_{H_0^*}$, M_1, and M_2 yielding the optimized DR in Fig. 1. Notice that P_d remains close to $1/e$ for $\rho_s \in [-8, 0]$ dB, not only for FXD, as predicted by (13), but also for TSD; in this region, the average scan time progressively reduces as ρ_s increases for all strategies: This is a consequence of the fact that stronger targets can be detected in a shorter time. Interestingly, for similar P_d values, TSD provides a shorter average scan time with respect to FXD, thus granting a DR gain: This is achieved by shortening the dwell time for each azimuth direction during the first observation (i.e., by reducing M_1) and by efficiently reinvesting part of the saved time for the revisits. As expected, for a reduced scan time, we must have a lower P_{fa} in order to maintain the same FAR level. If $\rho_s < -8$ dB, P_d gets progressively smaller for all detection strategies, since the dwell time is upper bounded. In this regime, both TSD and FXD use $M_{\max}$ pulses per
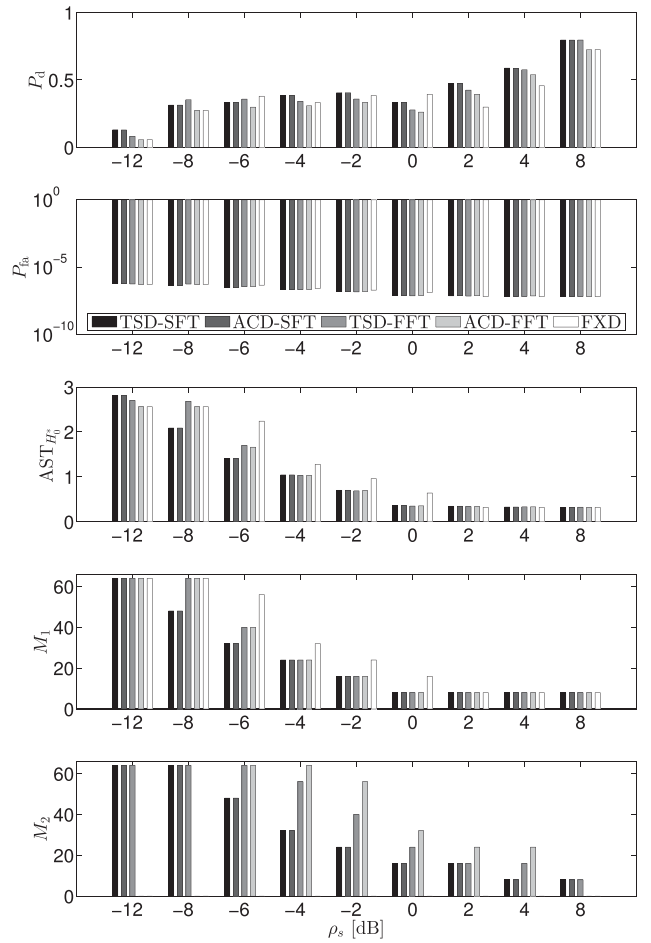

Fig. 2. P_d, P_{fa}, $\text{AST}_{H_0^*}$, M_1, and M_2 versus SNR per pulse yielding the optimized DR in Fig. 1 for TSD, ACD, and FXD when $N_a = 40$, $N_r = 1000$, $\text{FAR}_{\max} = 0.5$ fa/min, and $\rho_c = -\infty$ dB; both SFT and FFT are considered.

azimuth direction in the first look, while TSD may take advantage of the second look to possibly achieve a larger P_d: However, as ρ_s gets smaller, the improvement of P_d obtainable at the price of a longer scan time becomes less and less rewarding. If $\rho_s > 0$ dB, instead, P_d gets progressively larger for all detection strategies, since the dwell time is lower bounded. In this regime, both TSD and FXD use $M_{\min}$ pulses per azimuth direction in the first look, while TSD may take advantage of the second look to possibly achieve a larger P_d at the price of increasing the scan time: However, requesting a second look becomes less and less rewarding as ρ_s gets larger.

Figs. 3 and 4 show the optimized DR as a function of $\text{FAR}_{\max}$ (when $N_a = 40$, $N_r = 1000$, and $\rho_s = -4$ dB) and as a function of N_r (when $N_a = 40$, $\text{FAR}_{\max} = 0.5$ fa/min, and $\rho_s = -4$ dB), respectively. Again, it is verified by inspection that TSD outperforms FXD, while ACD remains in between; also, the performance corresponding to the SFT model is superior to that of the FFT model, in agreement with what shown in Fig. 1 at $\rho_s = -4$ dB. Notice that DR is an increasing function of $\text{FAR}_{\max}$ and a decreasing function of N_r for all detection strategies: This is a consequence of the fact that satisfying the FAR constraint is easier when
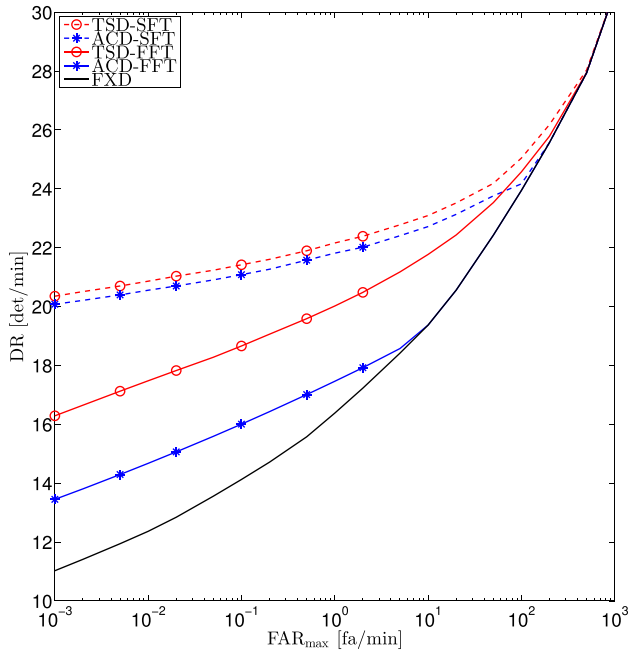
Fig. 3. Optimized DR versus FAR_{max} for TSD, ACD, and FXD when $N_a = 40$, $N_r = 1000$, $\rho_s = -4$ dB, and $\rho_c = -\infty$ dB; both SFT and FFT are considered.
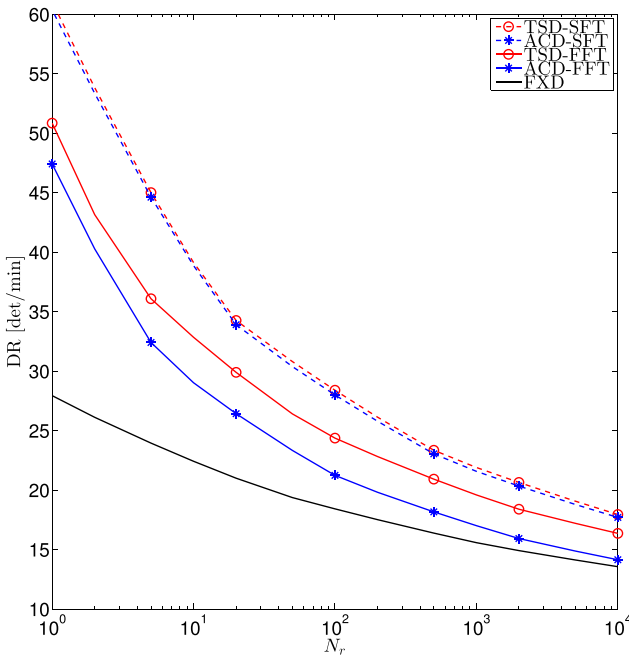

Fig. 4. Optimized DR versus N_r for TSD, ACD, and FXD when $N_a = 40$, $\text{FAR}_{\text{max}} = 0.5$ fa/min, $\rho_s = -4$ dB, and $\rho_c = -\infty$ dB; both SFT and FFT are considered.

FAR_{max} is increased and/or N_r reduced. This behavior is also explained by looking at Figs. 5 and 6, which report the values of P_d, P_{fa}, $\text{AST}_{H_0^*}$, M_1, and M_2 yielding the optimized DR in the corresponding Figs. 3 and 4, respectively. It is seen that, as FAR_{max} is increased (Fig. 5) or N_r decreased (Fig. 6), we may accept a larger P_{fa} and, hence, obtain a larger DR either by maintaining a similar P_d for a reduced scan time or by increasing P_d for a similar scan time. It is interesting that TSD and ACD become more and
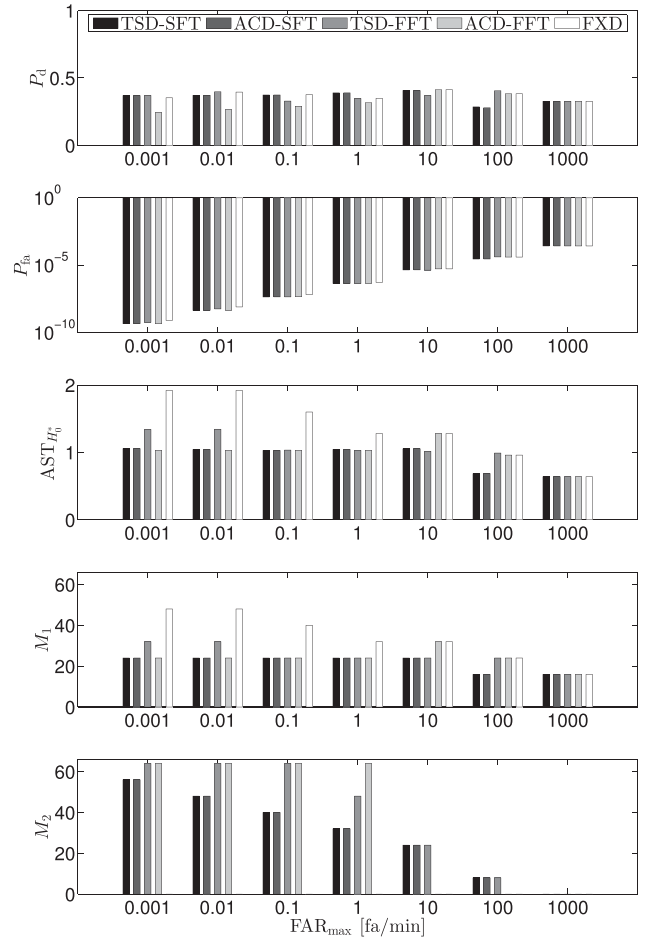

Fig. 5. P_d, P_{fa}, $\text{AST}_{H_0^*}$, M_1, and M_2 versus FAR_{max} yielding the optimized DR in Fig. 3 for TSD, ACD, and FXD when $N_a = 40$, $N_r = 1000$, $\rho_s = -4$ dB, and $\rho_c = -\infty$ dB; both SFT and FFT are considered.

more competitive with respect FXD as FAR_{max} or N_r is decreased. To further investigate this point, we analyze the sensitivity gain granted by TSD and ACD with respect to FXD. The sensitivity gain of a procedure A (either TSD or ACD) with respect to FXD at DR $= x$ is defined as[7]

$$G_s = \frac{\rho_s|_{\text{DR}=x \text{ for FXD}}}{\rho_s|_{\text{DR}=x \text{ for } A}}. \qquad (15)$$

In Fig. 7, we report G_s for TSD and ACD as a function of DR when $N_a = 40$ and $\rho_s = -4$ dB. Four configurations are considered: $\text{FAR}_{\text{max}} = 0.5$ fa/min and $N_r = 1000$ (top-left), $\text{FAR}_{\text{max}} = 0.5$ fa/min and $N_r = 100$ (top-right), $\text{FAR}_{\text{max}} = 0.05$ fa/min and $N_r = 1000$ (bottom-left), and $\text{FAR}_{\text{max}} = 0.05$ fa/min and $N_r = 100$ (bottom-right). Notice that the top-left subplot reproduces the sensitivity gain corresponding to the curves in Fig. 1. It is seen by inspection that G_s gets larger as N_r and/or FAR_{max} are decreased;

---

[7]For fixed transmit energy per pulse, ρ_s is proportional to the radar cross section (RCS) of the target, so that G_s measures the gain in terms of RCS (hence the name). Also, for fixed RCS, ρ_s is proportional to the transmit energy per pulse, so that, in the absence of clutter (where the disturbance is signal independent), G_s also measures the gain in transmit energy.
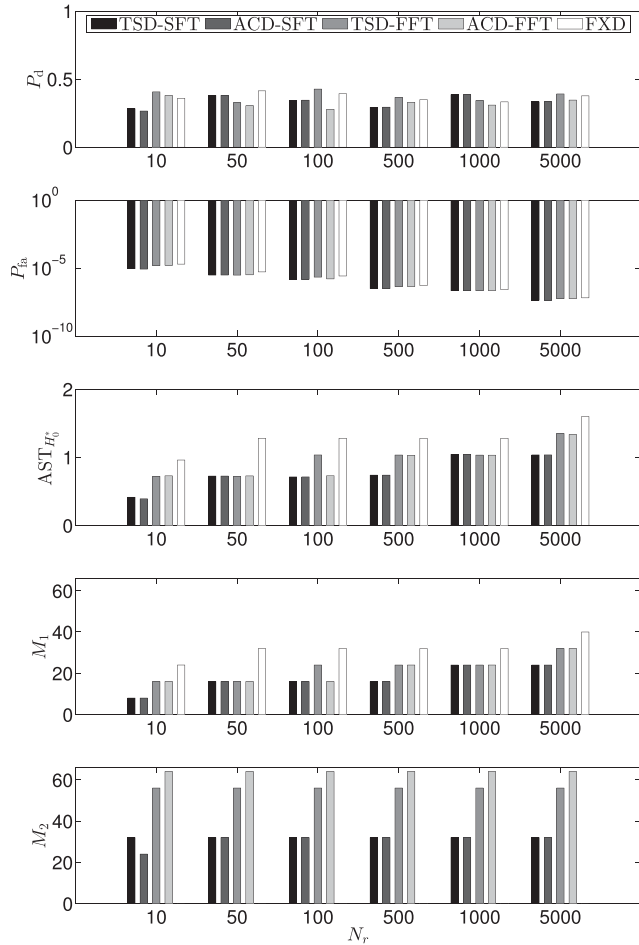
Fig. 6. P_d, P_{fa}, $AST_{H_0^*}$, M_1, and M_2 versus N_r yielding the optimized DR in Fig. 4 for TSD, ACD, and FXD when $N_a = 40$, $FAR_{max} = 0.5$ fa/min, $\rho_s = -4$ dB, and $\rho_c = -\infty$ dB; both SFT and FFT are considered.
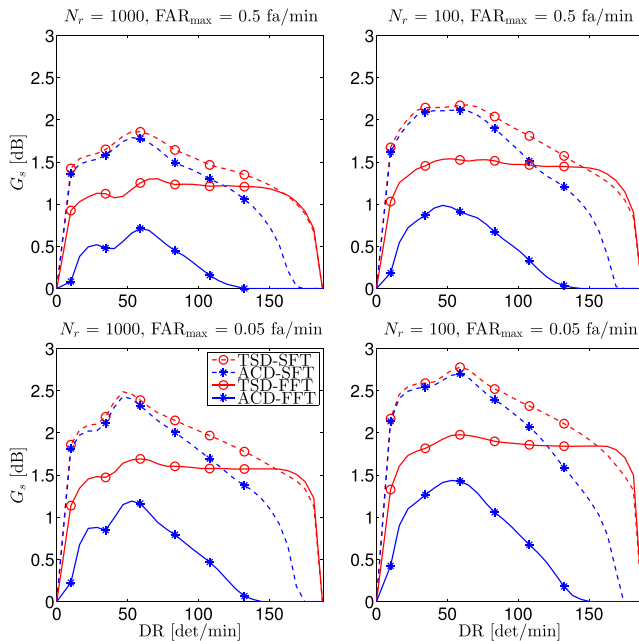

Fig. 7. Sensitivity gain granted by TSD and ACD with respect to FXD versus DR when $N_a = 40$, $N_r = 100$ or 1000, $FAR_{max} = 0.5$ or 0.05 fa/min, and $\rho_c = -\infty$ dB; both SFT and FFT are considered.
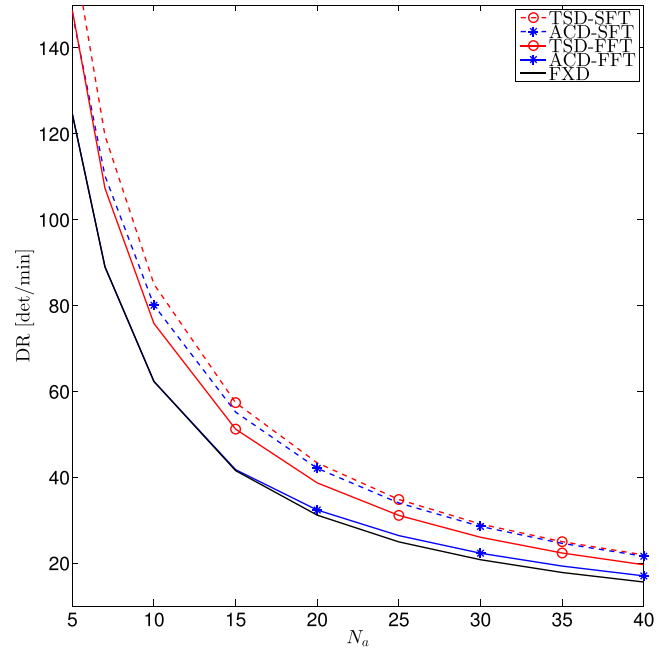

Fig. 8. Optimized DR versus N_a for TSD, the ACD, and FXD when $N_r = 1000$, $FAR_{max} = 0.5$ fa/min, $\rho_s = -4$ dB; and $\rho_c = -\infty$ dB; both SFT and FFT are considered.

in the two extreme scenarios (top-left and bottom-right) a gain of at most 1.8 and 2.8 dB, respectively, can be achieved by TSD over a wide DR range.

Figs. 8 and 9 show the optimized DR and the corresponding values of P_d, P_{fa}, $AST_{H_0^*}$, M_1, and M_2, respectively, as a function of N_a when $N_r = 1000$, $FAR_{max} = 0.5$ fa/min, and $\rho_s = -4$ dB. It is seen that the P_d and P_{fa} remain approximatively unaltered in the inspected range of N_a for all detection strategies; on the other hand, increasing the number of azimuth directions to be monitored requires to proportionally extend the duration of the scan; hence, DR approximatively scales as $1/N_a$ for all detection strategies. As regards the comparison among the performance of TSD, ACD, and FXD, considerations similar to those done in previous examples still apply here. Finally, Fig. 10 shows G_s for TSD and ACD as a function of DR for $N_a = 10, 20, 30$, or 40, $N_r = 1000$, $FAR_{max} = 0.5$ fa/min, and $\rho_s = -4$ dB. Notice that only DR values in the range $\left[0, 1/(N_a M_{min} T)\right]$ are achievable, whereby the curves for different N_a present a different support. Interestingly, the trend of the sensitivity gain granted by TSD inside the feasible DR range is similar for all inspected values of N_a.

B. Presence of Clutter

We now discuss the system performance in the presence of clutter. Fig. 11 shows the optimized DR as a function of ρ_c when $N_a = 40$, $N_r = 1000$, $FAR_{max} = 0.5$ fa/min, $\nu = 1$, and $\rho_s = -4$ dB, while Fig. 12 shows the corresponding values of P_d, P_{fa}, $AST_{H_0^*}$, M_1, and M_2. As expected, the optimized DR is a decreasing function of ρ_c, ranging from the noise-limited value observed in Fig. 1 to the lower bound $FAR_{max}/(N_r N_a)$. Interestingly, TSD remains
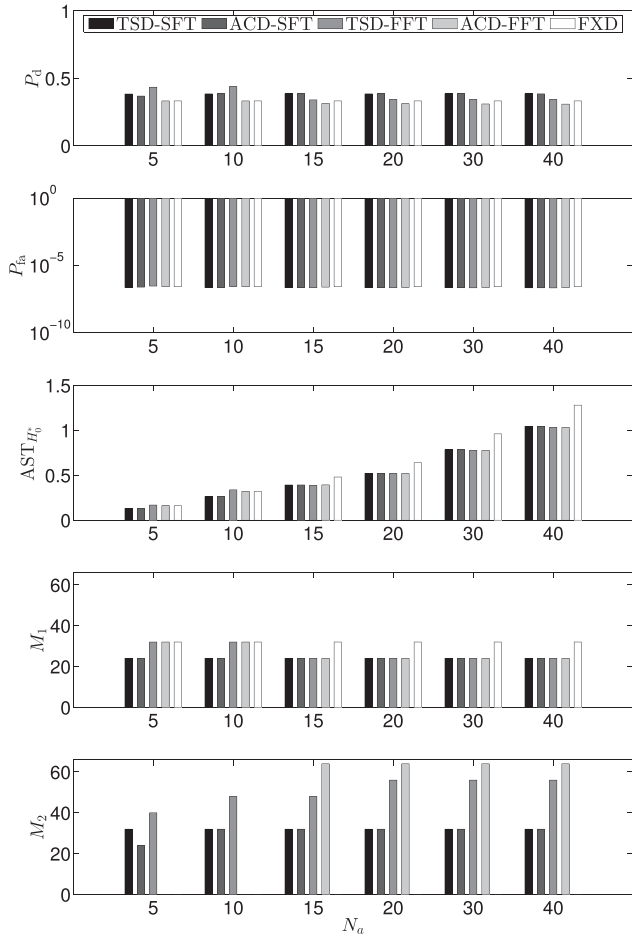
Fig. 9. P_d, P_{fa}, $\mathrm{AST}_{H_0^*}$, M_1, and M_2 versus N_a yielding the optimized DR in Fig. 8 for TSD, ACD, and FXD when $N_r = 1000$, $\mathrm{FAR}_{max} = 0.5$ fa/min, $\rho_s = -4$ dB, and $\rho_c = -\infty$ dB; both SFT and FFT are considered.
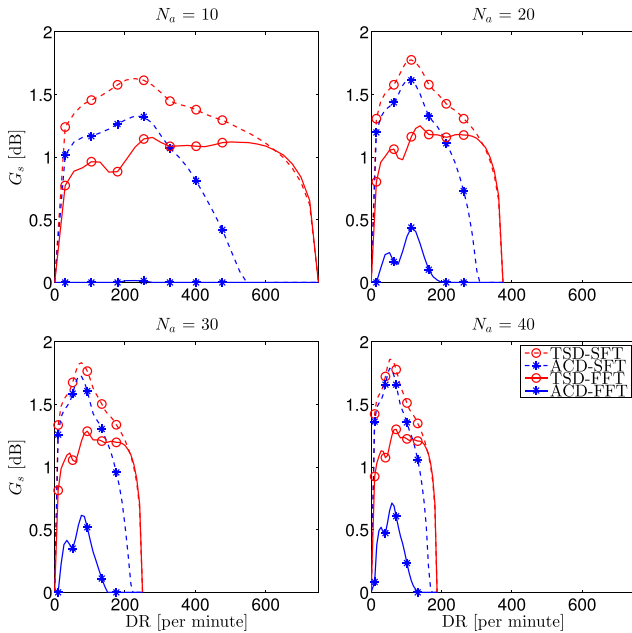
Fig. 10. Sensitivity gain granted by TSD and ACD with respect to FXD versus DR when $N_a = 10$, 20, 30, or 40, $N_r = 1000$, $\mathrm{FAR}_{max} = 0.5$ fa/min, and $\rho_c = -\infty$ dB; both SFT and FFT are considered.

Fig. 11. Optimized DR versus CRN per pulse for TSD, ACD, and FXD when $N_a = 40$, $N_r = 1000$, $\mathrm{FAR}_{max} = 0.5$ fa/min, $\nu = 1$, and $\rho_s = -4$ dB; both SFT and FFT are considered.

Fig. 12. P_d, P_{fa}, $\mathrm{AST}_{H_0^*}$, M_1, and M_2 versus CNR per pulse yielding the optimized DR in Fig. 11 for TSD, ACD, and FXD when $N_a = 40$, $N_r = 1000$, $\mathrm{FAR}_{max} = 0.5$ fa/min, $\nu = 1$, and $\rho_s = -4$ dB; both SFT and FFT are considered.
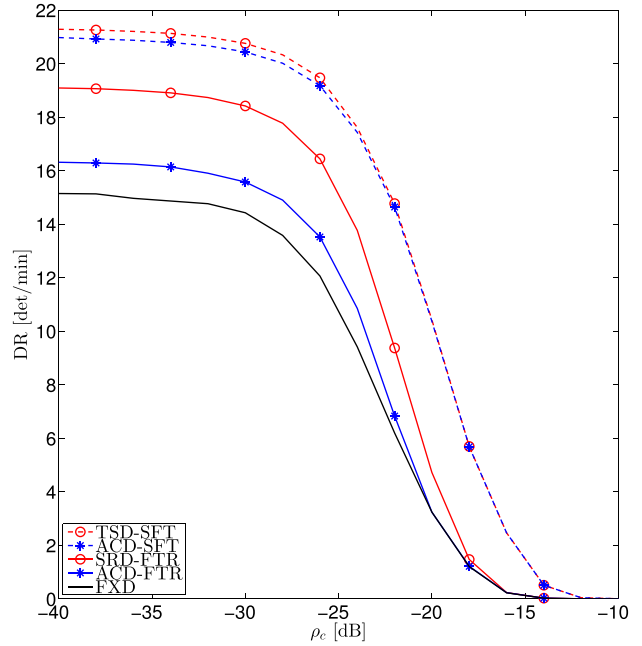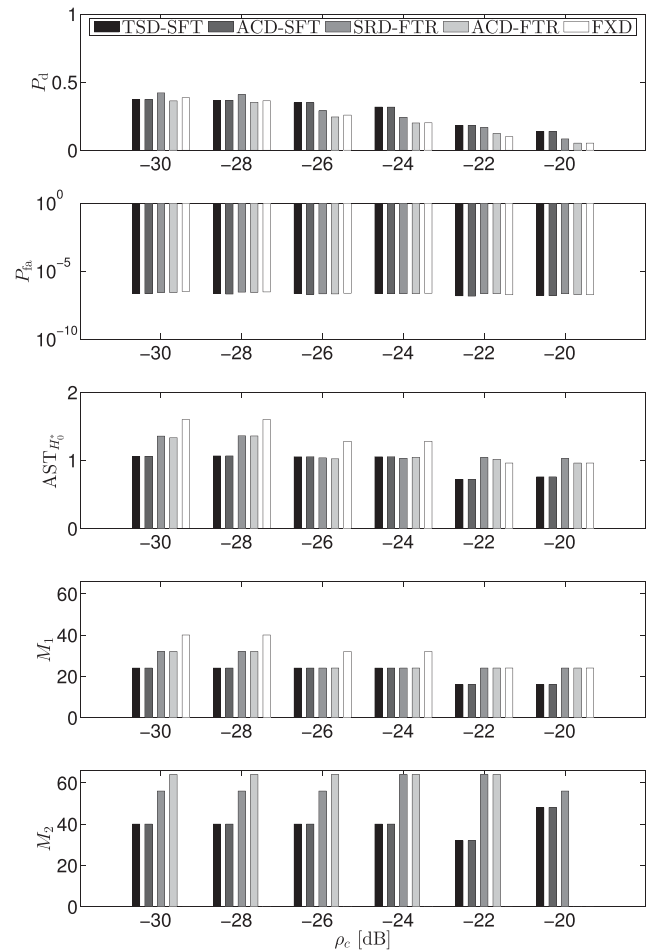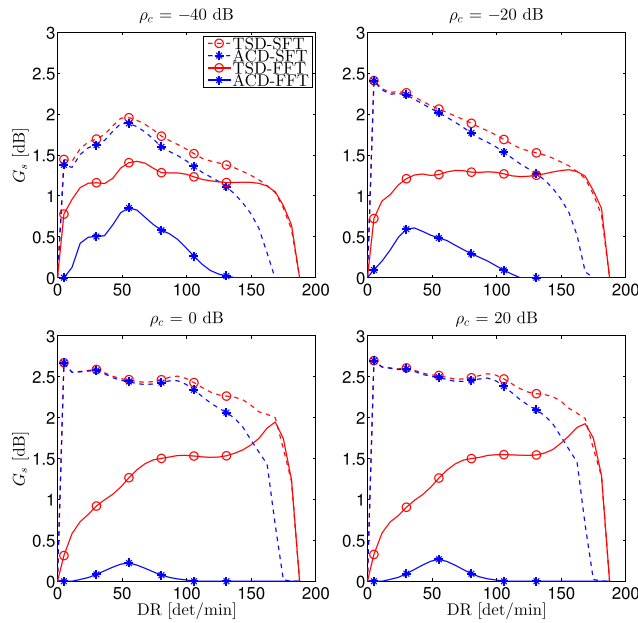
Fig. 13. Sensitivity gain granted by TSD and ACD with respect to FXD versus DR when $\rho_c = -40, -20, 0,$ or 20 dB, $N_a = 40$, $N_r = 1000$, $\text{FAR}_{\max} = 0.5$ fa/min, and $\nu = 1$; both SFT and FFT are considered.

significantly superior to FXD also in the clutter-limited regime, especially under the SFT model. To farther investigate this point, we study in Fig. 13 the sensitivity gain for TSD and ACD as a function of DR when $\rho_c = -40, -20, 0$ or 20 dB, $N_a = 40$, $N_r = 1000$, $\text{FAR}_{\max} = 0.5$ fa/min, $\nu = 1$, and $\rho_s = -4$ dB.

Under the SFT model, G_s for TSD increases with ρ_c, thus showing that a second look is even more rewarding in the presence of clutter. For example, at DR $= 30$ det/min, the gain is 1.70, 2.26, 2.58, and 2.61 dB for $\rho_c = -40, -20, 0, 20$ dB, respectively. As also observed in Figs. 7 and 10, TSD and ACD provide very close performance for small DR values (which correspond to low SCNR's); indeed, in this regime, TSD rarely declares a detection after the first observation. Instead, TSD and ACD have a quite different behavior for large DR values (which correspond to high SCNR's), since requesting a second look for strong targets is inefficient.

Under the FFT model, instead, G_s for TSD is a decreasing function of ρ_c at small DR values, while greatly increases at large DR values. The former behavior follows from the fact that, as the SCNR decreases, the probability of declaring a detection after the first observation reduces; also, a revisit triggered by an occasionally favorable target response s_1 becomes less effective, since the second look experiences an independent target response s_2, which is likely to be not favorable (recall also that the clutter texture remains constant during the scan). On the other hand, as the SCNR increases, a detection is usually declared after the first observation; if not, a revisit triggered by an occasionally unfavorable target response is likely to produce a detection, as the second look experiences most of the time a favorable target response.

Finally, notice that the gap between TSD and ACD is now more evident and greatly increases with ρ_c at all DR values.

V. CONCLUSION

TSD is a simple strategy to improve the probability of detection or the cumulative probability of detection under a constraint on the probability of false alarm, which is readily implementable on existing surveillance radars equipped with an electronically scanned antenna. In this paper, we have investigated the value of this sensitivity improvement when time becomes a resource at stake, and new figures of merit accounting for its cost are employed for system optimization and performance assessment.

Specifically, we have considered a detection procedure that requests a second look of the inspected resolution cell whenever a reliable decision cannot be made after the first observation; this strategy is general enough to subsume as special cases both FXD adopted by most mechanical systems and ACD proposed for some agile-beam radars. At the design stage, we have selected the dwell time and the detection thresholds in order to maximize DR under a constraint on FAR. This optimization framework is motivated by the fact a larger DR reduces the reaction time of the radar system and may facilitate the subsequent track maintenance operation, while FAR impacts on the ability of a human operator and/or an automatic controller to perform a real-time elaboration of the hits produced by the detector; also, DR and FAR provide a baseline framework for comparing the performance of detection strategies involving different scanning policies.

Our results reveal that TSD may be unnecessary in the extremely low and extremely high SCNR regions. In all other cases, the sensitivity gain depends on the operating conditions. Remarkably, TSD is generally more effective if the target response does not change between the two observations (which is usually the case if the second look is taken immediately after the first one) and in the clutter limited regime; moreover, it becomes more rewarding as the desired FAR level or the number of inspected range cells are reduced. Finally, we found that ACD can be significantly worse than TSD, as it uses the time resource less efficiently.

APPENDIX

Here we report the proofs for the closed-form expressions given in Section III: Specifically, FAR in (4) is derived in Section A, DR in (6) is derived in Section B, and the average scan time in (8) is derived in Section C.

A. Computation of FAR

Let A_1 and A_2 be the number of false alarms from all range-azimuth bins produced by the first and the second

observation, respectively. Then, FAR is

$$\text{FAR} = \mathrm{E}\left[\frac{A_1 + A_2 \mathbb{1}_{\{K \geq 1\}}}{N_a M_1 T + K M_2 T} \mid H_0^*\right]$$

$$= \sum_{k=0}^{N_a} \frac{\mathrm{E}[A_1 \mid K = k, H_0^*]}{N_a M_1 T + k M_2 T} \Pr(K = k \mid H_0^*)$$

$$+ \sum_{k=1}^{N_a} \frac{\mathrm{E}[A_2 \mid K = k, H_0^*]}{N_a M_1 T + k M_2 T} \Pr(K = k \mid H_0^*) \quad (16)$$

where $\mathbb{1}_{\mathcal{A}}$ is the indicator function of the event $\mathcal{A}$. At this point, we need to find an expression for the two conditional expectations in (16). To this end, we introduce the variable Q_j indicating the number of range bins to be revisited in the jth azimuth direction, for $j = 1, \ldots, N_a$. Then $Q_j \mid H_0^* \sim \mathcal{B}(N_r, p)$, where $\mathcal{B}(n, \theta)$ denotes the Binomial distribution with parameters $n \in \mathbb{N}$ and $\theta \in [0, 1]$. In the following, we treat separately the cases $p \in (0, 1)$, $p = 0$, and $p = 1$.

When $p \in (0, 1)$, the expectation of A_1 given that k azimuth directions are revisited is

$$\mathrm{E}[A_1 \mid K = k, H_0^*]$$

$$= \sum_{\ell_1=1}^{N_r} \cdots \sum_{\ell_k=1}^{N_r} \mathrm{E}[A_1 \mid Q_1 = \ell_1, \ldots, Q_k = \ell_k$$

$$Q_{k+1} = 0, \ldots, Q_{N_a} = 0, H_0^*]$$

$$\times \prod_{i=1}^{k} \Pr(Q_i = \ell_i \mid Q_i \geq 1, H_0^*)$$

$$= \sum_{\ell_1=1}^{N_r} \cdots \sum_{\ell_k=1}^{N_r} \left(N_r N_a - \sum_{j=1}^{k} \ell_j\right) \frac{P_{\text{fa},1}}{1 - p}$$

$$\times \prod_{i=1}^{k} \Pr(Q_i = \ell_i \mid Q_i \geq 1, H_0^*)$$

$$= \left(N_r N_a \prod_{i=1}^{k} \sum_{\ell_i=1}^{N_r} \Pr(Q_i = \ell_i \mid Q_i \geq 1, H_0^*)\right.$$

$$- \sum_{j=1}^{k} \left(\prod_{\substack{i=1\\i \neq j}}^{k} \sum_{\ell_i=1}^{N_r} \Pr(Q_i = \ell_i \mid Q_i \geq 1, H_0^*)\right.$$

$$\left.\left.\times \sum_{\ell_j=1}^{N_r} \ell_j \Pr(Q_j = \ell_j \mid Q_j \geq 1, H_0^*)\right)\right) \frac{P_{\text{fa},1}}{1 - p}$$

$$= \left(N_r N_a - k \mathrm{E}[Q_1 \mid Q_1 \geq 1, H_0^*]\right) \frac{P_{\text{fa},1}}{1 - p}$$

$$= \left(N_r N_a - \frac{k N_r p}{1 - (1 - p)^{N_r}}\right) \frac{P_{\text{fa},1}}{1 - p} \quad (17)$$

for $k = 0, \ldots, N_a$, where the first equality follows from the fact that the test statistics are independent and identically

distributed (i.i.d.), the second from

$$A_1 \mid \{Q_1 = \ell_1, \ldots, Q_k = \ell_k$$

$$Q_{k+1} = 0, \ldots, Q_{N_a} = 0, H_0^*\}$$

$$\sim \mathcal{B}\left(N_r N_a - \sum_{j=1}^{k} \ell_j, \frac{P_{\text{fa},1}}{1-p}\right) \quad (18)$$

the third from the fact that, for any function f and integers $\{J_i\}_{i=1}^{k}$, we have

$$\sum_{j_1=1}^{J_1} \cdots \sum_{j_k=1}^{J_k} \prod_{i=1}^{k} f(j_i) = \prod_{i=1}^{k} \sum_{j_i=1}^{J_i} f(j_i) \quad (19)$$

the fourth from

$$\sum_{i=1}^{N_r} \Pr(Q_i = \ell_i \mid Q_i \geq 1, H_0^*) = 1 \quad (20)$$

and the fact that $Q_j \mid \{Q_j \geq 1, H_0^*\}$ are identically distributed, and the last from

$$Q_1 \mid \{Q_1 \geq 1, H_0^*\} \sim \mathcal{B}\left(N_r, \frac{p}{1-(1-p)^{N_r}}\right). \quad (21)$$

Similarly, the expectation of A_2 given that k azimuth directions are revisited is

$$\mathrm{E}[A_2 \mid K = k, H_0^*]$$

$$= \sum_{\ell_1=1}^{N_r} \cdots \sum_{\ell_k=1}^{N_r} \mathrm{E}[A_2 \mid Q_1 = \ell_1, \ldots, Q_k = \ell_k$$

$$Q_{k+1} = 0, \ldots, Q_{N_a} = 0, H_0^*]$$

$$\times \prod_{i=1}^{k} \Pr(Q_i = \ell_i \mid Q_i \geq 1, H_0^*)$$

$$= \sum_{\ell_1=1}^{N_r} \cdots \sum_{\ell_k=1}^{N_r} \frac{P_{\text{fa},2}}{p} \sum_{j=1}^{k} \ell_j$$

$$\times \prod_{i=1}^{k} \Pr(Q_i = \ell_i \mid Q_i \geq 1, H_0^*)$$

$$= \frac{P_{\text{fa},2}}{p} \sum_{j=1}^{k} \left(\prod_{\substack{i=1\\i \neq j}}^{k} \sum_{\ell_i=1}^{N_r} \Pr(Q_i = \ell_i \mid Q_i \geq 1, H_0^*)\right.$$

$$\left.\times \sum_{\ell_j=1}^{N_r} \ell_j \Pr(Q_j = \ell_j \mid Q_j \geq 1, H_0^*)\right.$$

$$= \frac{k P_{\text{fa},2}}{p} \mathrm{E}[Q_1 \mid Q_1 > 0, H_0^*]$$

$$= \frac{k N_r P_{\text{fa},2}}{1 - (1 - p)^{N_r}} \quad (22)$$

for $k = 1, \ldots, N_a$, where the first equality follows from the fact that the test statistics are i.i.d., the second from

$$A_2 \mid \{Q_1 = \ell_1, \ldots, Q_k = \ell_k$$

$$Q_{k+1} = 0, \ldots, Q_{N_a} = 0, H_0^*\} \sim \mathcal{B}\left(\sum_{j=1}^{k} \ell_j, \frac{P_{\text{fa},2}}{p}\right)$$

$$\quad (23)$$

the third from (19), the fourth from (20), and the fact that $Q_j \mid \{Q_j \geq 1, H_0^*\}$ are identically distributed, and the last from (21). Then, plugging (17) and (22) in (16), we obtain

$$
\begin{aligned}
\text{FAR} = \sum_{k=0}^{N_a} & \frac{\left(N_r N_a - \frac{k N_r p}{1-(1-p)^{N_r}}\right) \frac{P_{\text{fa},1}}{1-p} + \frac{k N_r P_{\text{fa},2}}{1-(1-p)^{N_r}}}{N_a M_1 T + k M_2 T} \\
& \times \binom{N_a}{k} \left(1 - (1-p)^{N_r}\right)^k (1-p)^{N_r(N_a-k)} \quad (24)
\end{aligned}
$$

where we have exploited the fact that

$$
K \mid H_0^* \sim \mathcal{B}\left(N_a, 1 - (1-p)^{N_r}\right). \tag{25}
$$

Observe that $(k N_r p)/\left(1 - (1-p)^{N_r}\right)$ represents the average number of revisited cells given that $K = k$ azimuth directions are revisited, so that

$$
\frac{k N_r P_{\text{fa},2}}{1 - (1-p)^{N_r}} = \frac{k N_r p}{1 - (1-p)^{N_r}} \frac{P_{\text{fa},2}}{p} \tag{26a}
$$

$$
\left(N_r N_a - \frac{k N_r p}{1 - (1-p)^{N_r}}\right) \frac{P_{\text{fa},1}}{1-p} \tag{26b}
$$

in (24) are the average number of false alarms from revisited and nonrevisited cells, respectively, given that $K = k$.

If $p = 0$, no second look is taken under H_0^*, so that $A_1 \mid H_0^* \sim \mathcal{B}(N_a N_r, P_{\text{fa},1})$, $A_2 = 0$, and

$$
\text{FAR} = \text{E}\left[\frac{A_1}{N_a M_1 T} \mid H_0^*\right] = \frac{N_r P_{\text{fa},1}}{M_1 T}. \tag{27}
$$

On the other hand, if $p = 1$, all resolution cells are revisited under H_0^*, so that $A_1 = 0$, $A_2 \sim \mathcal{B}(N_a N_r, P_{\text{fa}})$, with $P_{\text{fa}} = P_{\text{fa},2} = \Pr(y_2 \geq \eta \mid H_0)$, and

$$
\text{FAR} = \text{E}\left[\frac{A_2}{N_a M_1 T + N_a M_2 T} \mid H_0^*\right] = \frac{N_r P_{\text{fa}}}{(M_1 + M_2)T}. \tag{28}
$$

B. Computation of DR

Let y_1 and y_2 be the statistics of the cell containing the target, and let D be a random variable taking on values 1, if the target is detected, and 0, otherwise, so that $D \sim \mathcal{B}(P_{\text{d}}, 1)$. Then, DR is

$$
\begin{aligned}
\text{DR} &= \text{E}\left[\frac{D}{N_a M_1 T + K M_2 T} \mid H_1^*\right] \\
&= \sum_{k=0}^{N_a} \text{E}\left[\frac{D}{N_a M_1 T + K M_2 T} \mid y_1 \notin [a, b) \right.
\end{aligned}
$$
$$
\left. K = k, H_1^* \right] \Pr\left(y_1 \notin [a, b), K = k \mid H_1^*\right)
$$

$$
\begin{aligned}
&+ \sum_{k=1}^{N_a} \text{E}\left[\frac{D}{N_a M_1 T + K M_2 T} \mid y_1 \in [a, b) \right. \\
&\left. K = k, H_1^* \right] \Pr\left(y_1 \in [a, b), K = k \mid H_1^*\right) \\
&= \sum_{k=0}^{N_a} \frac{\Pr\left(y_1 \geq b \mid y_1 \notin [a, b), K = k, H_1^*\right)}{N_a M_1 T + k M_2 T} \\
&\quad \times \Pr\left(y_1 \notin [a, b), K = k \mid H_1^*\right) \\
&+ \sum_{k=1}^{N_a} \frac{\Pr\left(y_2 \geq \eta \mid y_1 \in [a, b), K = k, H_1^*\right)}{N_a M_1 T + k M_2 T} \\
&\quad \times \Pr\left(y_1 \in [a, b), K = k \mid H_1^*\right) \\
&= \sum_{k=0}^{N_a} \frac{\Pr\left(y_1 \geq b, K = k \mid H_1^*\right)}{N_a M_1 T + k M_2 T} \\
&+ \sum_{k=1}^{N_a} \frac{\Pr\left(y_1 \in [a, b), y_2 \geq \eta, K = k \mid H_1^*\right)}{N_a M_1 T + k M_2 T}. \quad (29)
\end{aligned}
$$

At this point, we need to find the probabilities in the two summations.

Consider the case $p \in (0, 1)$, and let F be the event that the azimuth of the target needs a second look. The probability of detecting the target during the first observation and revisiting k azimuths is

$$
\begin{aligned}
\Pr(y_1 &\geq b, K = k \mid H_1^*) \\
&= P_{\text{d},1} \Pr\left(K = k \mid y_1 \geq b, H_1^*\right) \\
&= P_{\text{d},1} \Pr\left(K = k \mid F, y_1 \geq b, H_1^*\right) \\
&\quad \times \Pr(F \mid y_1 \geq b, H_1^*) \\
&\quad + P_{\text{d},1} \Pr\left(K = k, \mid \bar{F}, y_1 \geq b, H_1^*\right) \\
&\quad \times \Pr(\bar{F} \mid y_1 \geq b, H_1^*) \\
&= P_{\text{d},1} \Pr\left(K = k \mid F, H_1^*\right) \Pr(F \mid y_1 \geq b, H_1^*) \\
&\quad + P_{\text{d},1} \Pr\left(K = k, \mid \bar{F}, H_1^*\right) \Pr(\bar{F} \mid y_1 \geq b, H_1^*) \\
&= P_{\text{d},1} \binom{N_a - 1}{k - 1} \left(1 - (1-p)^{N_r}\right)^{k-1} \\
&\quad \times (1-p)^{N_r(N_a-k)} \left(1 - (1-p)^{N_r-1}\right) \mathbb{1}_{\{k \geq 1\}} \\
&\quad + P_{\text{d},1} \binom{N_a - 1}{k} \left(1 - (1-p)^{N_r}\right)^k \\
&\quad \times (1-p)^{N_r(N_a-1-k)} (1-p)^{N_r-1} \mathbb{1}_{\{k \leq N_a-1\}} \quad (30)
\end{aligned}
$$

for $k = 0, \ldots, N_a$, where $(\bar{\cdot})$ denotes negation and the last equality follows from:

$$
K - 1 \mid \{F, H_1^*\} \sim \mathcal{B}\left(N_a - 1, 1 - (1-p)^{N_r}\right) \tag{1}
$$
$$
K \mid \{\bar{F}, H_1^*\} \sim \mathcal{B}\left(N_a - 1, 1 - (1-p)^{N_r}\right) \tag{2}
$$
$$
\Pr(F \mid y_1 \geq b, H_1^*) = 1 - (1-p)^{N_r-1}. \tag{3}
$$

On the other hand, the probability of detecting the target during the second observation and revisiting k

azimuths is

$$\Pr\left(y_1 \in [a, b), y_2 \geq \eta, K = k \mid H_1^*\right)$$
$$= \Pr\left(y_1 \in [a, b), y_2 \geq \eta \mid H_1^*\right)$$
$$\times \Pr\left(K = k, \mid y_1 \in [a, b), H_1^*\right)$$
$$= P_{d,2}\binom{N_a - 1}{k - 1}\left(1 - (1 - p)^{N_r}\right)^{k-1}(1 - p)^{N_r(N_a - k)}$$
(32)

for $k = 1, \ldots, N_a$, where (7b) and (31a) have been exploited in the last equality (if $y_1 \in [a, b)$, then F is true). Then, plugging (30) and (32) in (29), DR becomes

$$\text{DR} = P_{d,1}(1 - p)^{N_r - 1}\sum_{k=0}^{N_a - 1}\binom{N_a - 1}{k}$$
$$\times \frac{\left(1 - (1 - p)^{N_r}\right)^k (1 - p)^{N_r(N_a - 1 - k)}}{N_a M_1 T + k M_2 T}$$
$$+ \left[P_{d,1}\left(1 - (1 - p)^{N_r - 1}\right) + P_{d,2}\right]$$
$$\times \sum_{k=1}^{N_a}\binom{N_a - 1}{k - 1}\frac{\left(1 - (1 - p)^{N_r}\right)^{k-1}(1 - p)^{N_r(N_a - k)}}{N_a M_1 T + k M_2 T}$$
$$= \sum_{k=0}^{N_a - 1}\left(\frac{P_{d,1}(1 - p)^{N_r - 1}}{N_a M_1 T + k M_2 T}\right.$$
$$+ \left.\frac{P_{d,1}\left(1 - (1 - p)^{N_r - 1}\right) + P_{d,2}}{N_a M_1 T + (k + 1)M_2 T}\right)$$
$$\times \binom{N_a - 1}{k}\left(1 - (1 - p)^{N_r}\right)^k (1 - p)^{N_r(N_a - 1 - k)}.$$
(33)

It might be interesting to notice that, in (33), $P_{d,1}(1 - p)^{N_r - 1}$ is the probability of detecting the target in the first look and not revisiting its azimuth direction; similarly, $P_{d,1}\left(1 - (1 - p)^{N_r - 1}\right)$ is the probability of detecting the target in the first look and revisiting its azimuth direction.

If $p = 0$, noise cells are never revisited, so that

$$\Pr(y_1 \geq b, K = k \mid H_1^*) = P_{d,1}\mathbb{1}_{\{k=0\}} \quad (34a)$$
$$\Pr\left(y_1 \in [a, b), y_2 \geq \eta, K = k \mid H_1^*\right) = P_{d,2}\mathbb{1}_{\{k=1\}} \quad (34b)$$

which, plugged in (29), give

$$\text{DR} = \frac{P_{d,1}}{N_a M_1 T} + \frac{P_{d,2}}{N_a M_1 T + M_2 T}.$$
(35)

On the other hand, if $p = 1$, noise cells are always revisited, so that

$$\Pr(y_1 \geq b, K = k \mid H_1^*) = \begin{cases} P_{d,1}\mathbb{1}_{\{k=N_a\}}, & \text{if } N_r \geq 2 \\ P_{d,1}\mathbb{1}_{\{k=N_a - 1\}}, & \text{if } N_r = 1 \end{cases}$$
(36a)
$$\Pr\left(y_1 \in [a, b), y_2 \geq \eta, K = k \mid H_1^*\right) = P_{d,2}\mathbb{1}_{\{k=N_a\}}$$
(36b)

which, plugged in (29), give

$$\text{DR} = \begin{cases} \dfrac{P_d}{N_a(M_1 + M_2)T}, & \text{if } N_r \geq 2 \\ \dfrac{P_{d,1}}{N_a M_1 T + (N_a - 1)M_2 T} + \dfrac{P_{d,2}}{N_a(M_1 + M_2)T}, & \text{if } N_r = 1. \end{cases}$$
(37)

C. Computation of the Average Scan Time

From (25)—which holds true for any value of p—, the average scan time under H_0^* is

$$\text{AST}_{H_0^*} = \text{E}[T_s \mid H_0^*]$$
$$= N_a M_1 T + \text{E}[K \mid H_0^*]M_2 T$$
$$= N_a M_1 T + N_a\left(1 - (1 - p)^{N_r}\right)M_2 T. \quad (38)$$

Similarly, exploiting (31)—which holds true for any value of p—, the average scan time under H_1^* is

$$\text{AST}_{H_1^*} = \text{E}[T_s \mid H_1^*]$$
$$= N_a M_1 T + \text{E}[K \mid H_1^*]M_2 T$$
$$= N_a M_1 T + \left(\text{E}[K \mid F, H_1^*]\Pr(F \mid H_1^*)\right.$$
$$+ \left.\text{E}[K \mid \bar{F}, H_1^*]\Pr(\bar{F} \mid H_1^*)\right)M_2 T$$
$$= N_a M_1 T + \left[\left(1 + (N_a - 1)\left(1 - (1 - p)^{N_r}\right)\right)\right.$$
$$\times \left(1 - (1 - q)(1 - p)^{N_r - 1}\right) + (N_a - 1)$$
$$\times \left.\left(1 - (1 - p)^{N_r}\right)(1 - q)(1 - p)^{N_r - 1}\right]M_2 T$$
$$= N_a M_1 T + \left[N_a\left(1 - (1 - p)^{N_r}\right)\right.$$
$$+ \left.(q - p)(1 - p)^{N_r - 1}\right]M_2 T. \quad (39)$$

REFERENCES

[1] P. A. Lynn
Radar Systems. New York, NY, USA: Van Nostrand, 1987.

[2] F. E. Nathanson, J. P. Reilly, and M. N. Cohen
Radar Design Principles: Signal Processing and the Environment.
Mendham, NJ, USA: SciTech Publishing, Inc., 1999.

[3] M. I. Skolnik
Introduction to Radar Systems. New York, NY, USA: McGraw-Hill, 2001.

[4] S. Blackman and R. Popoli
Design and Analysis of Modern Tracking Systems. Boston, MA, USA: Artech House, 1999.

[5] J. Clarke
Airborne early warning radar
Proc. IEEE, vol. 73, no. 2, pp. 312–324, Feb. 1985.

[6] D. K. Barton and S. A. Leonov
Radar Technology Encyclopedia. New York, NY, USA: Artech House, 1997.

[7] E. R. Billam
Phased array radar and the detection of 'low observables'
In *Proc. IEEE Int. Radar Conf.*, Arlington, VA, USA, May 1990, pp. 491–495.

[8] E. R. Billam
The problem of time in phased array radar
In *Proc. Radar 97 (IEE Conf. Publ. No. 449)*, Edinburgh, U.K., Oct. 1997, pp. 563–575.

[9] S. Miranda, C. Baker, K. Woodbridge, and H. Griffiths
Knowledge-based resource management for multifunction radar: A look at scheduling and task prioritization
IEEE Signal Process. Mag., vol. 23, no. 1, pp. 66–76, Jan. 2006.

[10] S. Miranda, C. Baker, K. Woodbridge, and H. Griffiths
Comparison of scheduling algorithms for multifunction radar
IET Radar, Sonar Navig., vol. 1, no. 6, pp. 414–424, Dec. 2007.

[11] V. Krishnamurthy and D. V. Djonin
Optimal threshold policies for multivariate POMDPs in radar
resource management
IEEE Trans. Signal Process., vol. 57, no. 10, pp. 3954–3969,
Oct. 2009.

[12] Z. Spasojevic, S. Dedeo, and R. Jensen
Dwell scheduling algorithms for phased array antenna
IEEE Trans. Aerosp. Electron. Syst., vol. 49, no. 1, pp. 42–54,
Jan. 2013.

[13] E. Grossi, M. Lops, and L. Venturino
A new look at the radar detection problem
IEEE Trans. Signal Process., vol. 64, no. 3, pp. 5835–5847,
Nov. 15, 2016.

[14] J. Arnold, S. Shaw, and H. Pasternack
Efficient target tracking using dynamic programming
IEEE Trans. Aerosp. Electron. Syst., vol. 29, no. 1, pp. 44–56,
Jan. 1993.

[15] S. M. Tonissen and Y. Bar-Shalom
Maximum likelihood track-before-detect with fluctuating target
amplitude
IEEE Trans. Aerosp. Electron. Syst., vol. 34, no. 3, pp. 796–806,
Jul. 1998.

[16] H. Im and T. Kim
Optimization of multiframe target detection schemes
IEEE Trans. Aerosp. Electron. Syst., vol. 35, no. 1, pp. 176–187,
Jan. 1999.

[17] S. J. Davey, M. G. Rutten, and B. Cheung
A comparison of detection performance for several track-
before-detect algorithms
In *Proc. Int. Conf. Inf. Fusion.*, Cologne, Germany, 2008, pp. 1–
8.

[18] E. Grossi, M. Lops, and L. Venturino
A novel dynamic programming algorithm for track-before-
detect in radar systems
IEEE Trans. Signal Process., vol. 61, no. 10, pp. 2608–2619,
May 2013.

[19] E. Grossi, M. Lops, and L. Venturino
A heuristic algorithm for track-before-detect with thresholded
observations in radar systems
IEEE Signal Process. Lett., vol. 20, no. 8, pp. 811–813,
Aug. 2013.

[20] E. Grossi, M. Lops, and L. Venturino
A track-before-detect algorithm with thresholded observations
and closely-spaced targets
IEEE Signal Process. Lett., vol. 20, no. 12, pp. 1171–1174,
Dec. 2013.

[21] E. Grossi, M. Lops, and L. Venturino
Track-before-detect for multiframe detection with censored ob-
servations
IEEE Trans. Aerosp. Electron. Syst., vol. 50, no. 3, pp. 2032–
2046, Jul. 2014.

[22] A. Aprile, E. Grossi, M. Lops, and L. Venturino
Track-before-detect for sea clutter rejection: tests with real data
IEEE Trans. Aerosp. Electron. Syst., vol. 54, no. 3, pp. 1035–
1045, Jun. 2016.

[23] G. van Keuk and S. S. Blackman
On phased-array radar tracking and parameter control
IEEE Trans. Aerosp. Electron. Syst., vol. 29, no. 1, pp. 186–194,
Jan. 1993.

[24] S. S. Blackman
Multiple hypothesis tracking for multiple target tracking
IEEE Trans. Aerosp. Electron. Syst., vol. 19, no. 1, pp. 5–18,
Jan. 2004.

[25] Y. Bar-Shalom, P. K. Willett, and X. Tian
Tracking and Data Fusion: A Handbook of Algorithms. Storrs,
CT, USA: YBS Publ., 2011.

[26] G. Zhang, S. Ferrari, and C. Cai
A comparison of information functions and search strategies
for sensor planning in target classification
IEEE Trans. Syst., Man Cybern.—Part B, Cybern., vol. 42,
no. 1, pp. 2–16, Feb. 2012.

[27] S. Watts
Performance measures for airborne maritime surveillance
radars
In *Proc. IEE Colloq. Specifying Meas. Perform. Modern
Radar Syst. (Ref. No. 1998/221)*, London, U.K., Mar. 1998,
pp. 9/1–9/6.

[28] S. S. Blackman
Multitarget tracking with an agile beam radar
In *Multitarget-Multisensor Tracking: Applications and Ad-
vances*, vol. II, Y. Bar-Shalom, Ed.
Norwood, MA, USA: Artech House, 1992.

[29] A. M. Kinghorn
Where next for airborne AESA technology?
IEEE Aerosp. Electron. Syst. Mag., vol. 24, no. 11, pp. 16–21,
Nov. 2009.

[30] P. J. Fielding and A. M. Kinghorn
Waveform optimisation for efficient resource allocation in air-
borne AESA radar systems
In *Proc. IEE Multifunction Radar Sonar Sensor Manage. Techn.
(Ref. No. 2001/173)*, Nov. 2001, pp. 3/1–3/6.

[31] A. Wald
Sequential Analysis. New York, NY, USA: Wiley, 1947.

[32] J. J. Bussgang and D. Middleton
Optimum sequential detection of signals in noise
IRE Trans. Inf. Theory, vol. 1, no. 3, pp. 5–18, Dec. 1955.

[33] C. W. Helstrom
A range-sampled sequential detection system
IRE Trans. Inf. Theory, vol. 8, no. 1, pp. 43–47, Jan. 1962.

[34] M. B. Marcus and P. Swerling
Sequential detection in radars with multiple resolution elements
IRE Trans. Inf. Theory, vol. 8, no. 4, pp. 237–245, Apr. 1962.

[35] I. S. Reed and I. Selin
A sequential test for the presence of a signal in one of k possible
positions
IEEE Trans. Inf. Theory, vol. 9, no. 4, pp. 286–288, Oct. 1963.

[36] R. Roberts
Sequential detection and composite hypotheses with applica-
tion to a signal of uncertain amplitude
IEEE Trans. Inf. Theory, vol. 13, no. 2, pp. 175–183, Apr. 1967.

[37] J. J. Bussgang
Sequential methods in radar detection
Proc. IEEE, vol. 58, no. 5, pp. 731–743, May 1970.

[38] W.-D. Wirth
Energy saving by coherent sequential detection of radar signals
with unknown doppler shift
IET Proc.—Radar, Sonar Navig., vol. 142, no. 3, pp. 145–152,
Jun. 1995.

[39] W.-D. Wirth
Radar Techniques Using Array Antennas (Radar, Sonar, Nav-
igation and Avionics Series), 2nd ed. London, U.K.: IET,
2013.

[40] S. Marano, V. Matta, and P. Willett
Sequential detection of almost-harmonic signals
IEEE Trans. Signal Process., vol. 51, no. 2, pp. 395–406,
Feb. 2003.

[41] A. G. Tartakovsky, X. R. Li, and G. Yaralov
Sequential detection of targets in multichannel systems
IEEE Trans. Inf. Theory, vol. 49, no. 2, pp. 425–445, Feb. 2003.

[42] E. Grossi and M. Lops
Sequential along-track integration for early detection of moving
targets
IEEE Trans. Signal Process., vol. 56, no. 8, pp. 3969–3982,
Aug. 2008.

[43] E. Grossi and M. Lops
Sequential detection of Markov targets with trajectory estimation
IEEE Trans. Inf. Theory, vol. 54, no. 9, pp. 4144–4154, Sep. 2008.

[44] E. Grossi and M. Lops
MIMO radar waveform design: A divergence-based approach for sequential and fixed-sample size tests
In *Proc. IEEE Int. Workshop Comput. Adv. Multi-Sensor Adapt. Process.*, Dec. 2009, pp. 165–168.

[45] E. Grossi and M. Lops
Space-time code design for MIMO detection based on Kullback-Leibler divergence
IEEE Trans. Inf. Theory, vol. 58, no. 6, pp. 3989–4004, Jun. 2012.

[46] M. Franceschetti, S. Marano, and V. Matta
Chernoff test for strong-or-weak radar models
IEEE Trans. Signal Process., vol. 65, no. 2, pp. 289–302, Jan. 2017.

[47] J. J. Bussgang and M. Marcus
Truncated sequential hypothesis tests
IEEE Trans. Inf. Theory, vol. 13, no. 3, pp. 512–516, Jul. 1967.

[48] N. D. Wallace
Design of truncated sequential tests for rapidly fading radar targets
IEEE Trans. Aerosp. Electron. Syst., vol. 4, no. 3, pp. 433–442, May 1968.

[49] S. Tantaratana and H. Poor
Asymptotic efficiencies of truncated sequential tests
IEEE Trans. Inf. Theory, vol. 28, no. 6, pp. 911–923, Nov. 1982.

[50] S. Tantaratana
Design of nonparametric truncated sequential detectors with parallel linear boundaries
IEEE Trans. Aerosp. Electron. Syst., vol. 25, no. 4, pp. 483–490, Jul. 1989.

[51] W. Zhang, G. V. Moustakides, and H. V. Poor
Opportunistic detection rules: Finite and asymptotic analysis
IEEE Trans. Inf. Theory, vol. 62, no. 4, pp. 2140–2152, Apr. 2016.

[52] H. M. Finn
A new approach to sequential detection in phased array radars
In *Proc. IEEE Nat. Winter Conv. Mil. Electron.*, Arlington, VA, USA, Jan./Feb. 1963.

[53] L. Brennan and F. Hill
A two-step sequential procedure for improving the cumulative probability of detection in radars
IEEE Trans. Mil. Electron., vol. 9, no. 3, pp. 278–287, Jul. 1965.

[54] G. A. van der Spek
Measured performance of a sequential two-step detection scheme
Proc. IEEE, vol. 60, no. 10, pp. 1242–1242, Oct. 1972.

[55] G. W. Stimson
Introduction to Airborne Radar. Mendham, NJ, USA: SciTech Publ., Inc., 1998.

[56] E. Grossi, M. Lops, and L. Venturino
A search-and-revisit scanning policy to improve the detection rate in agile-beam radars
In *Proc. IEEE Workshop Statist. Signal Process.*, Gold Coast, QLD, Australia, Jun. 2014, pp. 452–455.

[57] E. Grossi, M. Lops, and L. Venturino
Detection rate optimization in surveillance radars with two-step sequential detection
In *Proc. IEEE Int. Conf. Acoust., Speech Signal Process.*, New Orleans, LA, USA, Mar. 2017.

[58] A. Aprile, E. Grossi, M. Lops, and L. Venturino
A procedure to improve the detection rate in radar systems with an electronically-scanned antenna
In *Proc. Eur. Radar Conf.*, Rome, Italy, Oct. 2014, pp. 501–504.

Emanuele Grossi (M'08–SM'17) was born in Sora, Italy, on May 10, 1978. He received the Dr. Eng. degree in telecommunication engineering in 2002 and the Ph.D. degree in electrical engineering in 2006, both from the University of Cassino and Southern Lazio, Cassino, Italy.

In 2005, he was a Visiting Scholar in the Department of Electrical and Computer Engineering, University of British Columbia, Vancouver, BC, Canada, and in 2009, he had a visiting appointment in the Digital Technology Center, University of Minnesota, Minnesota, MN, USA. Since February 2006, he has been an Assistant Professor at the University of Cassino and Southern Lazio, Cassino, Italy. His research interests include wireless communication systems, radar detection and tracking, and statistical decision problems with emphasis on sequential analysis.

Marco Lops (M'96–SM'01) was born in Naples, Italy, on March 16, 1961. He received the Laurea degree in Electronic Engineering and the Ph.D. degree in Electronic and Computer Science Engineering from "Federico II" University, Naples, Italy, in 1986 and in 1992, respectively.

He was an Assistant (1989–1991) and an Associate Professor (1991–2000) with "Federico II" University. Since March 2000, he has been a Professor at University of Cassino and Southern Lazio, Cassino, Italy. In fall 2008, he was a Visiting Professor with the University of Minnesota, and in spring 2009, with Columbia University. During 2009–2011, he was also with ENSEEIHT, Toulouse, France. His research interests include detection and estimation, with emphasis on communications and radar signal processing.

Luca Venturino (S'03–M'06–SM'17) was born in Cassino, Italy, on August 26, 1979. He received the Ph.D. degree in electrical engineering from the University of Cassino and Southern Lazio, Cassino, Italy, in 2006.

In 2004 and 2009, he was a Visiting Researcher with Columbia University, New York, NY, USA. Between 2006 and 2008, he spent nine months in NEC Laboratories America, Princeton, NJ, USA. He is currently an Associate Professor at the University of Cassino and Southern Lazio. His research interests include detection, estimation, and resource allocation, with emphasis on communications and radar signal processing.